International Journal of Research in Engineering, Science and Management
Volume 4, Issue 4, April 2021
https://www.ijresm.com | ISSN (Online): 2581-5792

Heat Transfer Rates of Hydromagnetic Buoyancy Driven Turbulent Fluid Flow Over a Curved Surface

Wilys O. Mukuna*
Department of Mathematics and Computer Science, University of Kabianga, Kericho, Kenya

***Abstract*: In this paper an analysis of hydromagnetic turbulent fluid flow over an immersed curved surface is carried out. The curved surface was a circular infinite vertical cylinder. The fluid was considered to be electrically conducting while the surface was assumed to be insulated. The fluid flows along the axis of the cylinder. The flow is impulsively started and the flow problem analysed thereafter. A mathematical formulation of the problem is done using the conservation equations of momentum and energy. The Reynolds stress terms were resolved using Prandtl mixing length hypothesis. The arising governing nonlinear partial differential equations are subsequently presented as finite difference schemes and simulated using a computer programme. The results were presented graphically showing velocity and temperature profiles. The rates of heat transfer are presented in a table. It is observed that increase in both Grashof number and Prandtl number leads to an increase in rate of heat transfer.**

***Keywords*: Buoyancy, curved surface, Finite difference, Heat transfer, Hydromagnetic, Turbulent.**

1. Introduction

The study of fluid flow within a magnetic field is known as hydromagnetic or magnetohydrodynamics. This has been of great interest to scientists and engineers in recent years [5]. Most flows which occur in practical applications are turbulent. This term denotes a motion in which an irregular fluctuation is superimposed on the mainstream [9].

The effect of magnetic field on the turbulent wake of a cylinder in free-surface magnetohydrodynamic channel flow was studied by Rhoads *et al*, [7]. This was done in an MHD flow experiment detailing the modification of vortices in the wake of a circular cylinder. The axis of the cylinder was parallel to the applied magnetic field. From the results it was concluded that the reduction in effective viscosity was due to the surpression of small scale eddies by the magnetic field.

Nusselt number is a parameter equal to the dimensionless temperature gradient at the surface and it provides a measure of the convection heat transfer occurring at the surface [2].

Yoon *et. al.* [10] presented a numerical study on the fluid flow and heat transfer around a circular cylinder in an aligned magnetic field. In the study a two-dimensional laminar fluid flow and heat transfer past a circular cylinder in an aligned magnetic field was done using the spectral method. They concluded that as the intensity of applied magnetic field increased, the vortex shedding formed in the wake became weaker.

A numerical investigation of a hydromagnetic turbulent boundary layer fluid flow past a vertical infinite cylinder with Hall current was done by Mukuna *et. a.l* [6]. The flow was modeled using the momentum, energy and concentration conservation equations. The model equations were solved by a finite difference method. The effects of flow parameters on the primary velocity, secondary velocity, temperature and concentration profiles are investigated. The skin friction, rate of heat and mass transfer are computed and presented in tables. In the experiment the effect of Hall current on Primary velocity was not observed due to turbulence while there was decreased secondary velocity profile when Hall parameter wad increased.

Sarris *et al*, [8] carried out direct numerical simulations for the transient and turbulent natural convection cooling of an initially isothermal quiescent liquid metal placed in a vertical cylinder in the presence of a vertical magnetic field. The numerical results showed that the magnetic field had no observable effect at the initial stage of the vertical boundary layer development. They also observed that conduction heat transfer was favored during the transition stage.

The resultant pressure force acting on the surface of a volume partially or completely surrounded by one or more fluids under non flow conditions is defined as buoyant force and acts vertically on the volume. This force is equal to the weight of the displaced fluid and acts upwards through the centre of gravity of the displaced fluid [4].

Fluid can flow in a pipe, in a channel, in an enclosure or over a flat plate or a curved surface. A curved surface may be a cylinder, sphere or any other form of surface that is not flat. This study considers the flow of a fluid over an immersed circular cylindrical surface.

*Corresponding author: wmukunah@kabianga.ac.ke

Kanaris *et. al.* [3], studied a three-dimensional numerical simulation of magnetohydrodynamic flow around a confined circular cylinder under low, moderate, and strong magnetic fields. They presented results for values of the Hartmann number, based on the duct width, in the range of $0 \leq Ha \leq 1120$, and the Reynolds number, based on the cylinder diameter and centerline velocity, in the range $0 \leq Re \leq 5000$. The results revealed a non-monotonic dependence of the critical Reynolds number for the onset of vortex shedding, with respect to the Hartmann number. They also observed that there is an increase in the flow unsteadiness with increasing intensity of the magnetic field.

In this paper is presented an analysis of heat transfer rates of a hydromagnetic buoyancy driven turbulent fluid flow over an immersed curved surface. The curved surface is a circular vertical infinite cylinder.

2. Mathematical Formulation

We consider a two dimensional turbulent boundary layer flow. The fluid flow is along a vertical infinitely long cylinder lying in the x-y plane. The cylinder is immersed in the fluid. The axis of the cylinder is in the positive x-axis direction and the fluid flows upwards positive x-axis direction parallel to the axis of the cylinder. The cylinder is assumed to have non-end effects. The fluid is assumed incompressible and viscous. A strong magnetic field of uniform strength H_0 is applied along the x-axis. The induced magnetic field is considered negligible hence H = (0, 0, H_0). The temperature of the surface of the cylinder and the fluid are assumed to be the same initially. At time $t^*>0$ the fluid starts moving impulsively with velocity U_0 and at the same time the temperature of the cylinder is instantaneously raised to T_W^* which is maintained constant later on. Given that the flow is over a cylinder, cylindrical coordinate form of the governing equations are used. The flow is considered to be along the axial and angular components. There is no radial flow. Thus the two dimensions of this flow are x and θ.

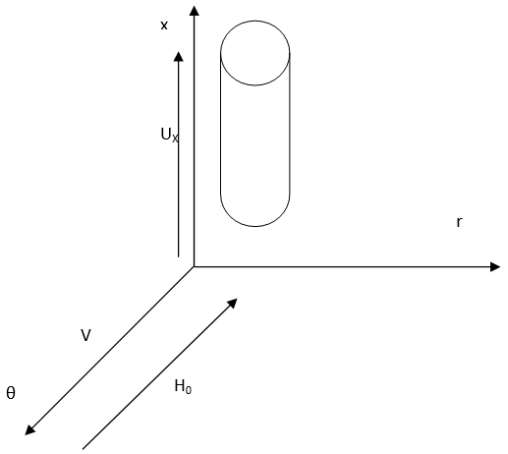

Fig. 1. Geometry of the problem

The above flow is governed by the following cylindrical coordinate equations:

$$\frac{\partial \overline{U}_x}{\partial t} = -\frac{1}{\rho}\frac{\partial \overline{P}}{\partial x} + \nu\left(\frac{\partial^2 U_x}{\partial r^2} + \frac{1}{r}\frac{\partial U_x}{\partial r}\right) - \left[\frac{1}{r}\frac{\partial \overline{U'_x U'_r}}{\partial r}\right] + \rho g + \vec{J} \times B\big|_x \quad \text{……..(1)}$$

$$\frac{\partial \overline{U_\theta^*}}{\partial t^*} = \nu\left(\frac{\partial^2 \overline{U_\theta^*}}{\partial r^{*2}} + \frac{1}{r^*}\frac{\partial \overline{U_\theta^*}}{\partial r^*} - \frac{\overline{U_\theta^*}}{r^{*2}}\right) - \left[\frac{\partial \overline{U'_r U'_\theta}}{\partial r^*} - \frac{2\overline{U'_\theta U'_r}}{r^*}\right] + \vec{J} \times B\big|_\theta \quad \text{……..(2)}$$

$$\rho C_p\left(\frac{\partial \overline{T^*}}{\partial t^*}\right) = k\left(\frac{\partial^2 \overline{T^*}}{\partial r^{*2}} + \frac{1}{r*}\frac{\partial \overline{T^*}}{\partial r^*}\right) - \rho C_p\left(\frac{\partial (\overline{U'_r T'})}{\partial r^*}\right) \quad \text{……..(3)}$$

It is noted that there is no pressure gradient in θ - direction and there is no gravitational force also. The boundary and initial conditions are:

$$t^* < 0 : U_x^* = 0, U_\theta^* = 0, T^* = T_\infty^*, \text{ everywhere} \quad \text{…….. (4)}$$

$$t^* \geq 0 : U_x^* = U_0, U_\theta^* = 0, T^* = T_W^*, \text{ at } r^* = \frac{D}{2} \text{ (D is the diameter of the cylinder.)} \quad \text{……(5)}$$

$$U_x^* \to 0, U_\theta^* \to 0, T^* \to T_\infty^*, \text{ as } r^* \to \infty \quad \text{……. ……(6)}$$

The pressure gradient in the x-axis direction results from the change in elevation up the cylinder. Thus:

$$\frac{\partial P}{\partial x} = -\rho_\infty g$$

Hence equation (1) becomes:

$$\rho\frac{\partial \overline{U}_x}{\partial t} = (\rho_\infty - \rho)g + \mu\left(\frac{\partial^2 U_x}{\partial r^2} + \frac{1}{r}\frac{\partial U_x}{\partial r}\right) - \rho\left[\frac{1}{r}\frac{\partial \overline{U'_x U'}_r}{\partial r}\right] + \vec{J}\times B\big|_x \quad \ldots\ldots\ldots\ldots\ldots\ldots(7)$$

The density difference $\rho - \rho_\infty$ may be expressed in terms of the volume coefficient of expansion β defined by:

$$\beta = \frac{1}{V}\left(\frac{\partial V}{\partial T}\right)_P = \frac{1}{V_\infty}\cdot\frac{V - V_\infty}{T - T_\infty} = \frac{\rho_\infty - \rho}{\rho(T - T_\infty)} \qquad \text{(Holman, [1])}$$

Such that (7) becomes

$$\rho\frac{\partial \overline{U}_x}{\partial t} = \rho\beta g(T - T_\infty) + \mu\left(\frac{\partial^2 U_x}{\partial r^2} + \frac{1}{r}\frac{\partial U_x}{\partial r}\right) - \rho\left[\frac{1}{r}\frac{\partial \overline{U'_x U'}_r}{\partial r}\right] + \vec{J}\times B\big|_x \quad \ldots\ldots\ldots\ldots\ldots\ldots(8)$$

Which simplifies to

$$\frac{\partial \overline{U}_x}{\partial t} = \beta g(T - T_\infty) + \nu\left(\frac{\partial^2 U_x}{\partial r^2} + \frac{1}{r}\frac{\partial U_x}{\partial r}\right) - \left[\frac{1}{r}\frac{\partial \overline{U'_x U'}_r}{\partial r}\right] + \vec{J}\times B\big|_x \quad \ldots\ldots\ldots\ldots\ldots\ldots(9)$$

Using (*) to indicate dimension, equation (9) becomes.

$$\frac{\partial \overline{U_x^*}}{\partial t^*} = \beta g(T^* - T_\infty^*) + \nu\left(\frac{\partial^2 \overline{U_{x\,x}^*}}{\partial r^{*2}} + \frac{1}{r^*}\frac{\partial \overline{U_x^*}}{\partial r^*}\right) - \left[\frac{1}{r^*}\frac{\partial \overline{U'_x U'}_r}{\partial r^*}\right] + \vec{J}\times B\big|_x \quad \ldots\ldots\ldots\ldots\ldots\ldots (10)$$

Next, we seek to establish the components of the electromagnetic force term in (10) and (2) that is the term: $\vec{J}\times\vec{B}$

The equation of conservation of charge $\nabla . J = 0,$ gives $j_r = k$, a constant, where $\vec{J} = (j_r, j_\theta, j_z)$. The constant is zero since, $j_r = 0$ at the cylinder which is insulated. Thus $j_r = 0$ everywhere in the flow. Neglecting the ion-slip and thermoelectric effects, generalized Ohm's law including the effects of Hall current gives:

$$\vec{J} + \frac{w_e\tau_e}{H_0}(\vec{J}\times\vec{H}) = \sigma\left(\vec{E} + \mu_0\vec{q}\times\vec{H} + \frac{1}{en_e}\nabla P_e\right) \quad \ldots\ldots\ldots\ldots\ldots\ldots(11)$$

For the problem we seek to solve there is no applied electric field hence $\vec{E} = 0$ and thus neglecting electron pressure, equation (11) becomes:

$$\vec{J} + \frac{w_e\tau_e}{H_0}(\vec{J}\times\vec{H}) = \sigma\mu_0(\vec{q}\times\vec{H}) \quad \ldots\ldots\ldots\ldots\ldots\ldots(12)$$

Given that $\vec{H} = (H_0, 0, 0)$ and taking $\vec{J} = (0, j_{\theta,} j_x)$, $\vec{q} = (0, U_\theta, U_x)$ and $\vec{B} = \mu_0\vec{H}$ simplifying equation (12) and solving gives:

$$j_r = 0 \quad \ldots\ldots\ldots\ldots\ldots\ldots(13)$$

$$j_\theta = \frac{\sigma\mu_0 H_0(U_z + mU_\theta)}{1 + m^2} \quad \ldots\ldots\ldots\ldots\ldots\ldots(14)$$

$$j_z = \frac{\sigma\mu_0 H_0(mU_z - U_\theta)}{1 + m^2} \quad \ldots\ldots\ldots\ldots\ldots\ldots(15)$$

Where $m = w_e\tau_e$ is the Hall parameter.

Thus the electromagnetic force along θ and x-axis are respectively:

$$(J\times B)_\theta = \frac{\sigma\mu_0^2 H_0^2(mU_z - U_\theta)}{1 + m^2} \quad \ldots\ldots\ldots\ldots\ldots\ldots(16)$$

$$(J\times B)_x = \frac{-\sigma\mu_0^2 H_0^2(U_z + mU_\theta)}{1 + m^2} \quad \ldots\ldots\ldots\ldots\ldots\ldots(17)$$

Hence the governing equations (10) and (2) are respectively:

$$\frac{\partial \overline{U_x^*}}{\partial t^*} = \nu\left(\frac{\partial^2 \overline{U_x^*}_{x}}{\partial r^{*2}} + \frac{1}{r^*}\frac{\partial \overline{U_x^*}}{\partial r^*}\right) - \left[\frac{1}{r^*}\frac{\partial \overline{U_x' U_r'}}{\partial r^*}\right] + \beta g\left(T^* - T_\infty^*\right) - \frac{\sigma\mu_0^2 H_0^2(\overline{U_x^*} + m\overline{U_\theta^*})}{1+m^2} \quad \text{.....(18)}$$

$$\frac{\partial \overline{U_\theta^*}}{\partial t^*} = \nu\left(\frac{\partial^2 \overline{U_\theta^*}}{\partial r^{*2}} + \frac{1}{r^*}\frac{\partial \overline{U_\theta^*}}{\partial r^*} - \frac{\overline{U_\theta^*}}{r^{*2}}\right) - \left[\frac{\partial \overline{U_r' U_\theta'}}{\partial r^*} - \frac{2\overline{U_\theta' U_r'}}{r^*}\right] + \frac{\sigma\mu_0^2 H_0^2(m\overline{U_x^*} - \overline{U_\theta^*})}{1+m^2} \quad \text{.....(19)}$$

A. Non-Dimensionalization

We seek to non-dimensionalize equations (3), (18) and (19). The following scaling variables are applied in the non-dimensionalization process:

$$t = \frac{t^* U_0^2}{\nu}; r = \frac{r^* U_0}{\nu}; U_i = \frac{U_i^*}{U_0}; \theta = \frac{T^* - T_\infty^*}{T_w^* - T_\infty^*} \quad \text{.....(20)}$$

The (*) superscript denotes the dimensional variables, Uo is the reference velocity, D is the diameter of the cylinder, $T^*_w - T^*_\infty$ is the temperature difference between the surface and the free stream temperature.

Using the scaling variables above yields the following equations:

$$\frac{\partial U_x}{\partial t} = \left(\frac{\partial^2 U_x}{\partial r^2} + \frac{1}{r}\frac{\partial U_x}{\partial r}\right) - \left[\frac{1}{r}\frac{\partial \overline{U_x' U_r'}}{\partial r}\right] + Gr\theta - M^2\frac{(U_x + mU_\theta)}{(1+m^2)} \quad \text{.....(21)}$$

$$\frac{\partial U_\theta}{\partial t} = \left(\frac{\partial^2 U_\theta}{\partial r^2} + \frac{1}{r}\frac{\partial U_\theta}{\partial r} - \frac{U_\theta}{r^2}\right) - \left[\frac{\partial \overline{U_x' U_r'}}{\partial r} - \frac{2\overline{U_\theta' U_r'}}{r}\right] + M^2\frac{(mU_x - U_\theta)}{(1+m^2)} \quad \text{.....(22)}$$

$$\frac{\partial \theta}{\partial t} = \frac{1}{\Pr}\left(\frac{\partial^2 \theta}{\partial r^2} + \frac{1}{r}\frac{\partial \theta}{\partial r}\right) - \frac{\partial(\overline{U_r'' \theta'})}{\partial r} \quad \text{.....(23)}$$

Where:

$$Gr = \nu g\beta\frac{T_w^* - T_\infty^*}{U_0^3}$$

$\Pr = \mu C_p/k$

$$M^2 = \frac{\sigma\mu_0^2 H_0^2 \nu}{U_0^2}$$

B. Boundary and Initial Conditions

From equation (20) the non-dimensional form of (5) becomes:

$$t < 0 : U_x = 0, U_\theta = 0, \theta = 0 \text{ everywhere} \quad \text{.....(24)}$$

$$t \geq 0 : U_x = 1, U_\theta = 0, \theta = 1 \text{ at } r = \frac{1}{2} \quad \text{.....(25)}$$

$$U_x \to 0, U_\theta \to 0, \theta \to 0 \text{ as } r \to \infty \quad \text{.....(26)}$$

C. Prandtl Mixing Length Hypothesis

We need to solve equations (21), (22) and (23), subject to equations (24), (25) and (26). However the solution of these equations is not currently possible due to the Reynolds stress terms. We thus resolve these terms first, for us to be able to work out the approximate solution of these equations by a direct numerical method. The momentum equations are resolved using Prandtl mixing length hypothesis. The Reynolds stresses in the energy conservation equation are computed in terms of Turbulent Prandtl number and Prandtl mixing length hypothesis. Thus equations (21) – (26) become:

$$\frac{\partial U_x}{\partial t} = \left(\frac{\partial^2 U_x}{\partial r^2} + \frac{1}{r}\frac{\partial U_x}{\partial r}\right) + k^2 r\left(\frac{\partial U_x}{\partial r}\right)\left(\frac{\partial U_x}{\partial r}\right) + Gr\theta - M^2\frac{(U_x + mU_\theta)}{(1+m^2)} \quad \text{.....(27)}$$

$$\frac{\partial U_\theta}{\partial t}=\left(\frac{\partial^2 U_\theta}{\partial r^2}+\frac{1}{r}\frac{\partial U_\theta}{\partial r}-\frac{U_\theta}{r^2}\right)+2k^2r^2\left(\frac{\partial U_\theta}{\partial r}\right)\left(\frac{\partial^2 U_\theta}{\partial r^2}\right)+M^2\frac{(mU_x-U_\theta)}{(1+m^2)} \quad \text{.....(28)}$$

$$\frac{\partial \theta}{\partial t}=\frac{1}{\mathrm{Pr}}\left(\frac{\partial^2\theta}{\partial r^2}+\frac{1}{r}\frac{\partial\theta}{\partial r}\right)+\frac{k^2r^2}{\mathrm{Pr}_t}\left(\frac{\partial U_x}{\partial r}\right)\left(\frac{\partial\theta}{\partial r}\right) \quad \text{.....(29)}$$

$$t<0: U_x=0, U_\theta=0, \theta=0, \text{everywhere} \quad \text{.....(30)}$$

$$t\geq 0: U_x=1, U_\theta=0, \theta=1, \text{ at } r=\frac{1}{2} \quad \text{.....(31)}$$

$$U_x\to 0, U_\theta\to 0, \theta\to 0, \text{as } r\to\infty \quad \text{.....(32)}$$

D. Finite Difference Scheme

Considering that the systems of partial differential equations (27) – (29) are highly non-linear their solutions are approximated by finite difference method. In the following finite difference scheme the primary velocity U_x is denoted by U and the secondary velocity U_θ is denoted by V to reduce the subscripts as i and j are used as subscripts, i corresponding to r as j corresponds to t. The equivalent finite difference scheme for equations are respectively:

Where i and j refer to r and t respectively. r have been substituted with $i\Delta r$.

$$U_{(i,j+1)}=U_{(i,j)}+\Delta t\left(\frac{U_{(i+1,j)}-2U_{(i,j)}+U_{(i-1,j)}}{(\Delta r)^2}+\frac{1}{i\Delta r}\frac{U_{(i+1,j)}-U_{(i,j)}}{\Delta r}\right)+$$
$$k^2 i(\Delta r)(\Delta t)\left(\frac{U_{(i+1,j)}-U_{(i,j)}}{\Delta r}\right)^2+\Delta t\left\{Gr\theta_{(i,j)}-M^2\frac{(U_{(i,j)}+mV_{(i,j)})}{1+m^2}\right\} \quad \text{.....(33)}$$

$$V_{(i,j+1)}=V_{(i,j)}+\Delta t\left(\frac{V_{(i+1,j)}-2V_{(i,j)}+V_{(i-1,j)}}{(\Delta r)^2}+\frac{1}{i\Delta r}\frac{V_{(i+1,j)}-V_{(i,j)}}{\Delta r}-\frac{V_{(i,j)}}{(i\Delta r)^2}\right)+$$
$$2k^2(i\Delta r)^2(\Delta t)\left(\frac{V_{(i+1,j)}-V_{(i,j)}}{\Delta r}\right)\left(\frac{V_{(i+1,j)}-2V_{(i,j)}+V_{(i-1,j)}}{(\Delta r)^2}\right)+\Delta tM^2\frac{(mU_{(i,j)}-V_{(i,j)})}{1+m^2} \quad \text{.....(34)}$$

$$\theta_{(i,j+1)}=\theta_{(i,j)}+\frac{\Delta t}{\mathrm{Pr}}\left(\frac{\theta_{(i+1,j)}-2\theta_{(i,j)}+\theta_{(i-1,j)}}{(\Delta r)^2}+\frac{1}{i\Delta r}\frac{\theta_{(i+1,j)}-\theta_{(i,j)}}{\Delta r}\right)+$$
$$\frac{k^2(\Delta t)(i\Delta r)^2}{\mathrm{Pr}_t}\left(\frac{U_{(i+1,j)}-U_{(i,j)}}{\Delta r}\right)\left(\frac{\theta_{(i+1,j)}-\theta_{(i,j)}}{\Delta r}\right) \quad \text{.....(35)}$$

The boundary and initial conditions take the form:

$$j<0: U_{(i,j)}=0, V_{(i,j)}=0, \theta_{(i,j)}=0, \text{ everywhere} \quad \text{.....(36)}$$

$$j\geq 0: U_{(i,j)}=1, V(i,j)=0, \theta_{(i,j)}=1, \text{ at } i=\frac{\mathrm{Re}}{2} \quad \text{.....(37)}$$

$$U_{(i,j)}\to 0, V_{(i,j)}\to 0, \theta_{(i,j)}\to 0, \text{ as } i\to\infty \quad \text{.....(38)}$$

Using the boundary and initial conditions we compute values for consecutive grid points for primary velocity, secondary velocities, and temperature that is $U_{(i,j+1)}$, $V_{(i,j+1)}$ and $\theta_{(i,j+1)}$ in component form.

The approximate solution was computed using a computer programme and the results are displayed in graphs as shown in figures 2, 3 and 4.

E. Determination of the Rate of Heat Transfer

The rate of heat transfer is determined from the temperature profiles. This is given by:

$$Nu=-\frac{\partial\theta}{\partial r}_{r=0.5} \quad \text{.....(39)}$$

This was calculated by numerical differentiation using Newton's interpolation formula over the first five points as given in the following equation:

$$Nu = \frac{5}{6}\left[25\theta_{(0,i)} - 48\theta_{(1,i)} + 36\theta_{(2,i)} - 16\theta_{(3,i)} + 3\theta_{(4,i)}\right] \quad \text{.....(40)}$$

3. Discussion of Results

The simulation was considered when the Grashof number is greater than zero, $Gr = 1\times10^4$. In this case the cylinder is at a higher temperature than the surrounding leading to cooling of the cylinder by free convection currents resulting in buoyancy force.

A. Primary Velocity Profiles

From Figure 2 it is noted that:

(i) Primary velocity is not affected by magnetic parameter and Hall parameter.
(ii) There is an increase in primary velocity profiles when Grashof number and time parameter are increased.
(iii) There is no change in primary velocity when Prandtl is increased.

B. Secondary Velocity Profiles

From Figure 3 it is noted that:

(i) The secondary velocity profiles increase in magnitude with increase in time parameter and magnetic parameter.
(ii) Variation in Grashof number does not affect secondary velocity profiles
(iii) There is no variation in velocity profiles with variation in Prandtl number.
(iv) There is decrease in the secondary velocity profiles with increase in Hall parameter.

C. Temperature Profiles

From Figure 4 it is noted that:

(i) There is no observable variation in temperature profiles with variation in magnetic parameter and Hall parameter.
(ii) There is increase in temperature profiles with increase in time parameter.
(iii) There is decrease in temperature profiles with increase in Grashof number
(iv) Increase in Prandtl number leads to decrease in temperature profiles.

D. Heat Transfer Rates

From Table 1 it is observed that

i) Change in time does not affect the rate of heat transfer.
ii) Increase in Grashof number leads to an increase in heat transfer.
iii) Increase in Prandtl number leads to an increase in heat transfer.

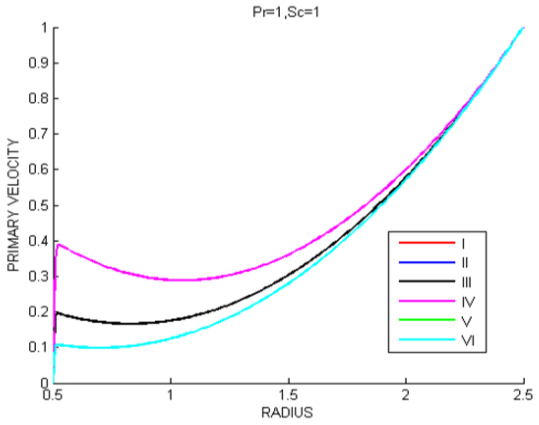

Fig. 2. Primary velocity profiles

	M^2	m	t	Gr	Grm
I	2	2	0.2	1.0E4	1.0E4
II	4	2	0.2	1.0E4	1.0E4
III	2	4	0.2	1.0E4	1.0E4
IV	2	2	0.4	1.0E4	1.0E4
V	2	2	0.2	1.0E3	1.0E4
VI	2	2	0.2	1.0E4	1.0E3

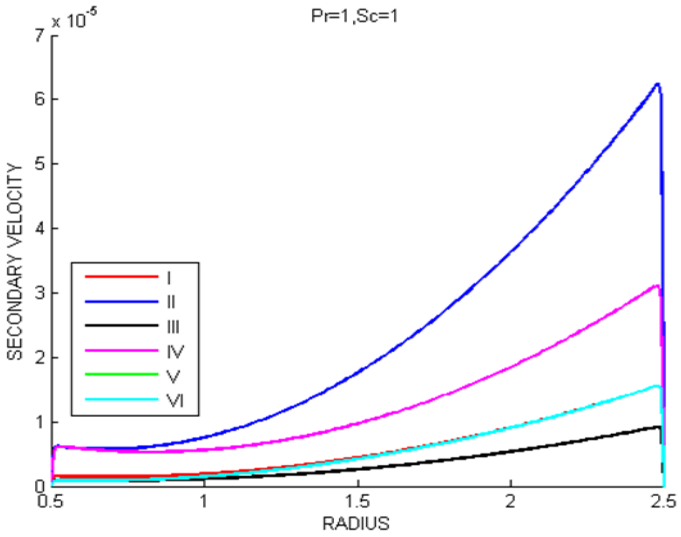

Fig. 3. Secondary velocity profiles

	M^2	m	t	Gr	Grm
I	2	2	0.2	1.0E4	1.0E4
II	4	2	0.2	1.0E4	1.0E4
III	2	4	0.2	1.0E4	1.0E4
IV	2	2	0.4	1.0E4	1.0E4
V	2	2	0.2	1.0E3	1.0E4
VI	2	2	0.2	1.0E4	1.0E3

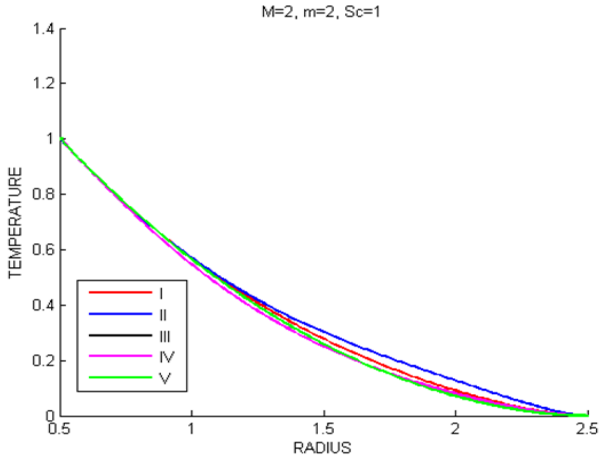

Fig. 4. Temperature profiles

	t	Gr	Grm	Pr
I	0.2	1.0E4	1.0E4	1
II	0.4	1.0E4	1.0E4	1
III	0.2	2.0E5	1.0E4	1
IV	0.4	1.0E4	2.0E5	1
V	0.2	1.0E3	1.0E4	10

Table 1
Heat transfer rates

	t	Gr	Grm	Pr	Nu
I	0.2	1.0E4	1.0E4	1	-7.6082E-4
II	0.4	1.0E4	1.0E4	1	-7.6082E-4
III	0.2	2.0E5	1.0E4	1	-7.6447E-4
IV	0.4	1.0E4	2.0E5	1	-7.6447E-4
V	0.2	1.0E3	1.0E4	10	-2.4090E-4

4. Conclusion

An analysis of heat transfer rates of a hydromagnetic buoyancy driven turbulent flow of a conducting fluid over a curved surface is numerically studied. The effects of various flow parameters on the mean velocities and mean temperature are discussed. There was no observable change in Primary velocity with variation in Hall parameter while increase in Grashof number led to increase in the primary velocity. Secondary velocity profiles decreased with increase in Hall parameter while there was no observable variation in temperature profiles with variation in magnetic parameter and Hall parameter. Change in Prandtl number significantly varied the temperature profiles. Increase in both Grashof number and Prandtl number causes an increase in rate of heat transfer.

References

[1] Holman, J. P., (2010) *Heat transfer —10th ed*. Mcgraw-Hill series in mechanical engineering.
[2] Incropera F.P. and Dewitt D. P. (1990). Fundamentals of Heat and Mass Transfer. *New Jersy, John Wiley & Sons*
[3] Kanaris N., Albets X., Grigoriadis D. and Kassinos, S. (2013). Three-dimensional numerical simulations of magnetohydrodynamic flow around a confined circular cylinder under low, moderate, and strong magnetic fields, *Physics of Fluids*, 257, 1-29
[4] Kothandaraman C. P. and Rudramoorthy R. (2007). *Fluid mechanics and Machinery*, New Age International
[5] Kwanza J.K., Mukuna W. O. and Kinyanjui M (2010).; A mathematical model of turbulent convective fluid flow past a vertical infinite plate with Hall current*; International Journal of Modelling and Simulation, 30(3), 376- 386*
[6] Mukuna, W.O; Kwanza, J.K, Sigei J.K and Okello J.A. (2017). Modeling hydro-magnetic turbulent free convection fluid flow over an immersed infinite vertical cylinder. *World journal of engineering research and technology, 3(2), 218-234.*
[7] Rhoads J. R., Edlund E. M. and Ji H. (2014). Effect of magnetic field on the turbulent wake of a cylinder in free-surface magnetohydrodynamic channel flow. *Journal of Fluid Mechanics*, 742, 446-765
[8] Sarris E., Iatridis A. I., Dritselis C. D., and Vlachos N. S., (2010). Magnetic field effect on the cooling of a low-Pr fluid in a vertical cylinder, *Physics of Fluids*, 22, 98 - 113.
[9] Schlichting. H. And Gersten K., (2017). *Boundary layer theory*, Springer.
[10] Yoon H. S., Chun H. H., Ha M. Y., and Lee H. G., (2004) A numerical study on the fluid flow and heat transfer around a circular cylinder in an aligned magnetic field, *International Journal of Heat and Mass Transfer, 47, 4075 - 4083.*

Nomenclature

Symbol	Quantity
j	Current density, A/m^2
H	Magnetic field intensity, Wb/m^2
H_0	Constant magnetic field intensity, Wb/m^2
t	Time, s
E	Electric field, V/m
$U_r, \mathrm{U}_\theta, \mathrm{U}_\mathrm{x}$	Components of velocity in the r, θ, and x axes respectively, m/s
P	Pressure of the fluid, N/m^2
P_e	Pressure of the fluid, N/m^2
T	Absolute temperature, K
C_p	Specific heat at constant pressure of the fluid, $J/kg/K$
D	Characteristic diameter, m
r^*, θ^*, x^*	Dimensional cylindrical coordinates f the fluid,
ω_e	electron cyclotron frequency, Hz
t^*	Dimensional time, s
T^*	Dimensional temperature, K
T_∞^*	Temperature of the fluid in the free stream, K
T_w^*	Temperature of the fluid at the plate, K
U, V	Dimensionless mean velocity components in θ and r axes respectively,
t	Dimensionless time, s
M^2	Magnetic parameter
m	Hall parameter
Pr	Prandtl number
Pr_t	Turbulent Prandtl number

Greek symbols

Symbol	Quantity
ρ	Fluid density, kg/m^3
μ	Coefficient of viscosity, kg/ms
μ_0	Magnetic permeability, H/m
$\Delta t, \Delta r$	Time and distance intervals
ν	Kinematic viscosity, m^2/s
τ_e	Collision time of electron, s
θ	Dimensionless fluid temperature
σ	Electrical conductivity, $\Omega^{-1}\mathrm{m}^{-1}$ s